

Supporting Information

Formation of Insoluble Brown Carbon through Iron-Catalyzed Reaction of Biomass Burning Organics

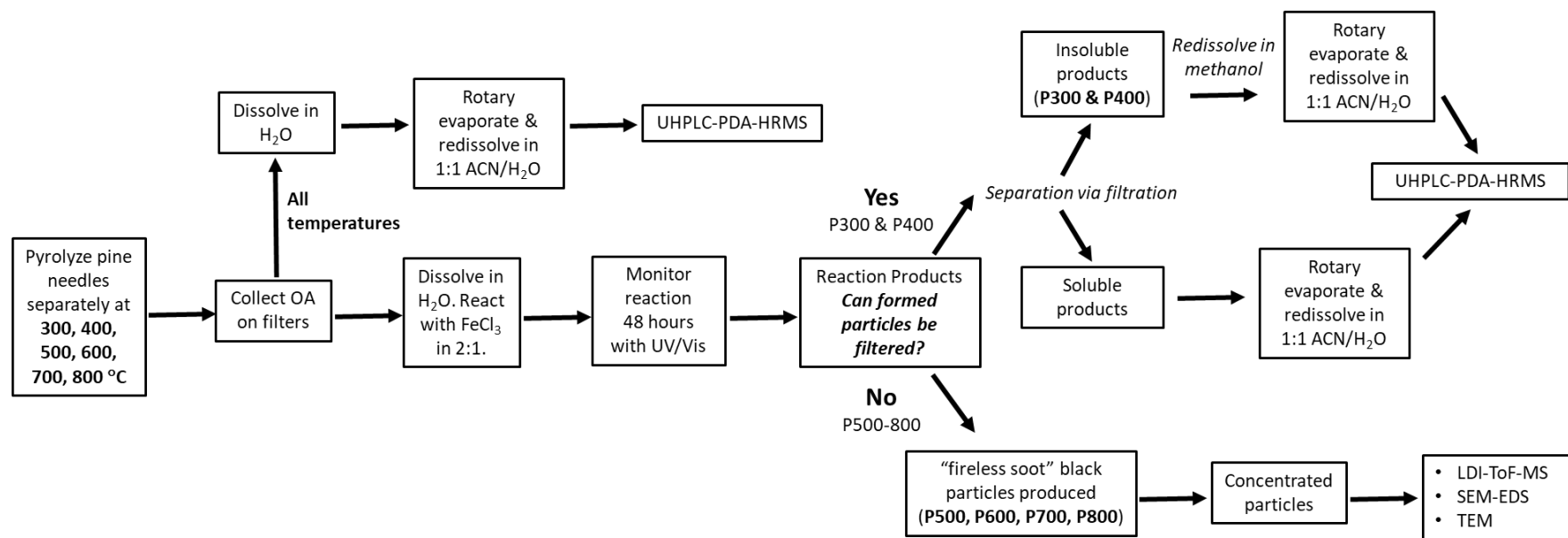
Katherine S. Hopstock¹, Brooke P. Carpenter¹, Joseph P. Patterson,¹ Hind A. Al-Abadleh², Sergey A. Nizkorodov¹

[1] Department of Chemistry, University of California, Irvine, Irvine, California 92697, USA.

[2] Department of Chemistry and Biochemistry, Wilfrid Laurier University, Waterloo, ON, Canada.

Table of Contents

<i>Scheme S1. Experimental flowchart of all temperature pyrolysis reactions and analysis methods.</i>	2
<i>Figure S1. Absorption spectra for the water-soluble OA fractions generated through the pyrolysis of Canary Island Pine needles.</i>	3
<i>Figure S2. Solutions of OA500-800 extracts 10 min after addition of FeCl₃.</i>	3
<i>Table S1. Summary of UHPLC-HRMS results from unreacted OA300-800 samples compared to the results for the water-insoluble products (P300 and P400) after reaction with FeCl₃.</i>	4
<i>Figure S3. Sample UHPLC-PDA-HRMS chromatograms of reaction products</i>	5
<i>Figure S4. Heat maps of UHPLC-PDA chromatograms as a function of absorption wavelength for unreacted, water-soluble OA</i>	6
<i>Figure S5. Mass spectra of OA500-800 samples run on UHPLC-PDA-HRMS prior to reaction with FeCl₃.</i> ...	7
<i>Figure S6. Laser desorption ionization time-of-flight mass spectrum (LDI-ToF-MS) for black water-insoluble particles.</i>	8
<i>Figure S7. Representative SEM and EDS data for polycatechol particles.</i>	9
<i>Figure S8. Representative SEM and EDS data for P600 (reaction particles) particles.</i>	9
<i>Table S2. List of compounds reproducibly detected by UHPLC-PDA-HRMS in negative ion mode from the pyrolysis of Canary Island Pine needles at 300-800 °C.</i>	10
References	16



Scheme S1. Experimental flowchart of all temperature pyrolysis reactions and analysis methods. Organic aerosol generated through pyrolysis is labeled as “OA” with its pyrolysis temperature listed after (i.e., OA300 is the organic aerosol generated through pyrolysis at 300 °C). The same label (e.g., OA300) is also used for the water-extracts of OA from the filters. Insoluble particles generated in the reactions of OA water extracts with Fe(III) are labeled as “P” with the pyrolysis temperature after (i.e., P300 are the insoluble particles generated through the reaction of OA300 with Fe(III)). All OA samples were analyzed with HRMS prior to reaction with iron (first upward arrow). Analysis methods for the reaction products were dictated by whether formed particles could be filtered out of the solution or not. In the case of P300 and P400, generated in OA300 + Fe(III) and OA400 + Fe(III) reactions, respectively, particles were sufficiently large to be separated from soluble reaction products by common filtration (pore size 0.22 μm) and were analyzed with HRMS. In the case of P500-800, black particles formed and were too small to be filtered. However, they could be centrifuged at 14,000 g for 10 minutes for imaging by TEM and SEM. In addition, dry residues of the suspensions of these particles were characterized by LDI-ToF-MS.

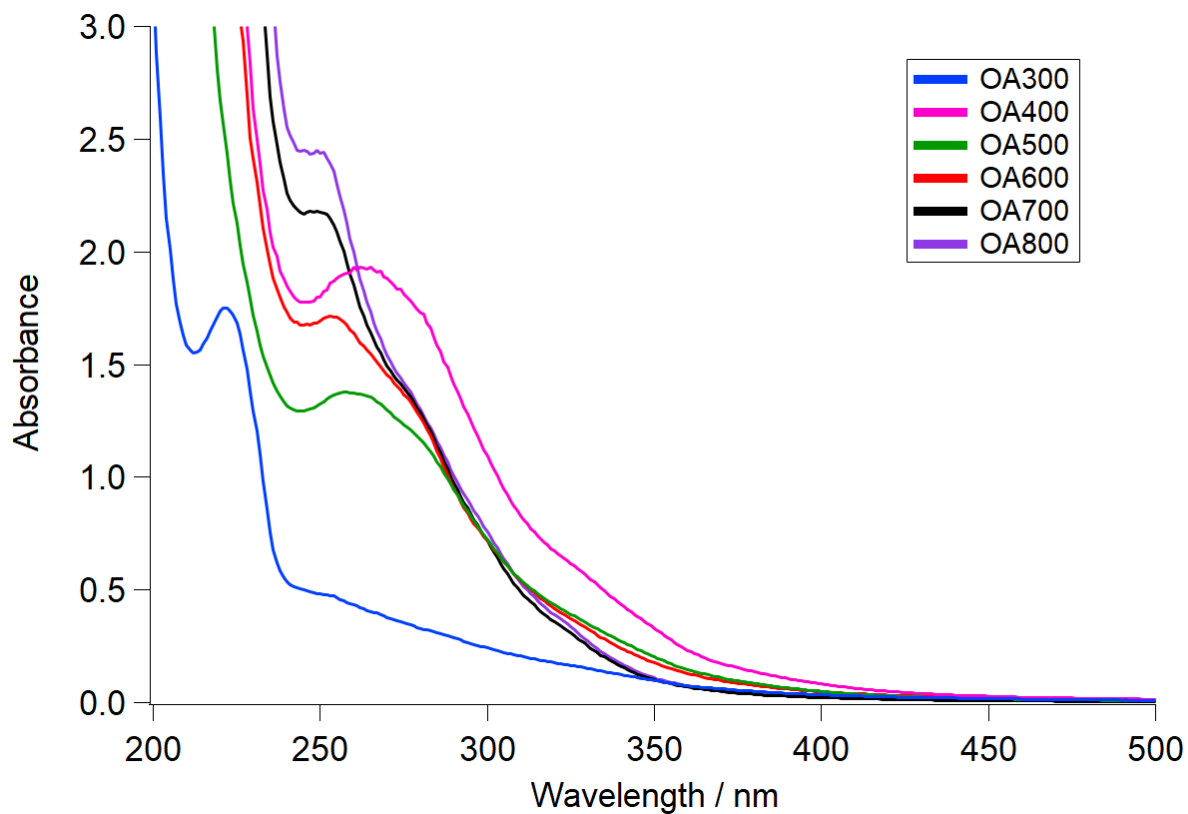


Figure S1. Absorption spectra for the water-soluble OA fractions generated through the pyrolysis of Canary Island Pine needles. The colors correspond to 300 °C (blue), 400 °C (pink), 500 °C (green), 600 °C (red), 700 °C (black), and 800 °C (purple) pyrolysis temperatures.

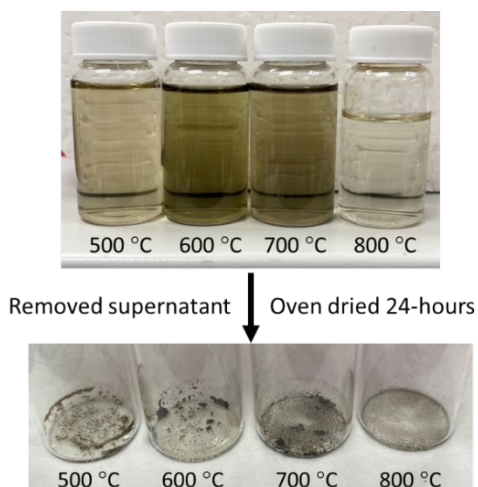


Figure S2. Solutions of OA500-800 extracts 10 min after addition of FeCl_3 . After reaction for 48 h, the generated particles settled to the bottom of the vials, and the supernatant was removed. The particles were suspended in a few mL of the solution and then dried in an oven for 24 h. These dried particles were then used for LDI-ToF-MS experiments.

Table S1. Summary of UHPLC-HRMS results from unreacted OA300-800 samples compared to the results for the water-insoluble products (P300 and P400) after reaction with FeCl₃. Similar data could not be obtained for P500-800 because particles were not soluble in most solvents.

Pyrolysis Temperature	Type of Sample	Average Molecular Weight	Average Neutral Molecular Formula	Average O:C
300 °C	Unreacted OA	324.9	C ₁₇ H ₂₀ O ₆	0.37 ± 0.19
	Water-insoluble products	486.1	C ₂₈ H ₄₁ O ₇	0.27 ± 0.16
400 °C	Unreacted OA	337.49	C ₁₇ H ₂₁ O ₇	0.43 ± 0.26
	Water-insoluble products	435.50	C ₂₄ H ₃₈ O ₇	0.30 ± 0.10
500 °C	Unreacted OA	299.04	C ₁₆ H ₁₉ O ₆	0.39 ± 0.18
	Water-insoluble products	-	-	-
600 °C	Unreacted OA	320.27	C ₁₇ H ₁₇ O ₆	0.36 ± 0.14
	Water-insoluble products	-	-	-
700 °C	Unreacted OA	316.19	C ₁₇ H ₁₆ O ₅	0.28 ± 0.12
	Water-insoluble products	-	-	-
800 °C	Unreacted OA	313.02	C ₁₆ H ₁₀ O ₅	0.32 ± 0.13
	Water-insoluble products	-	-	-

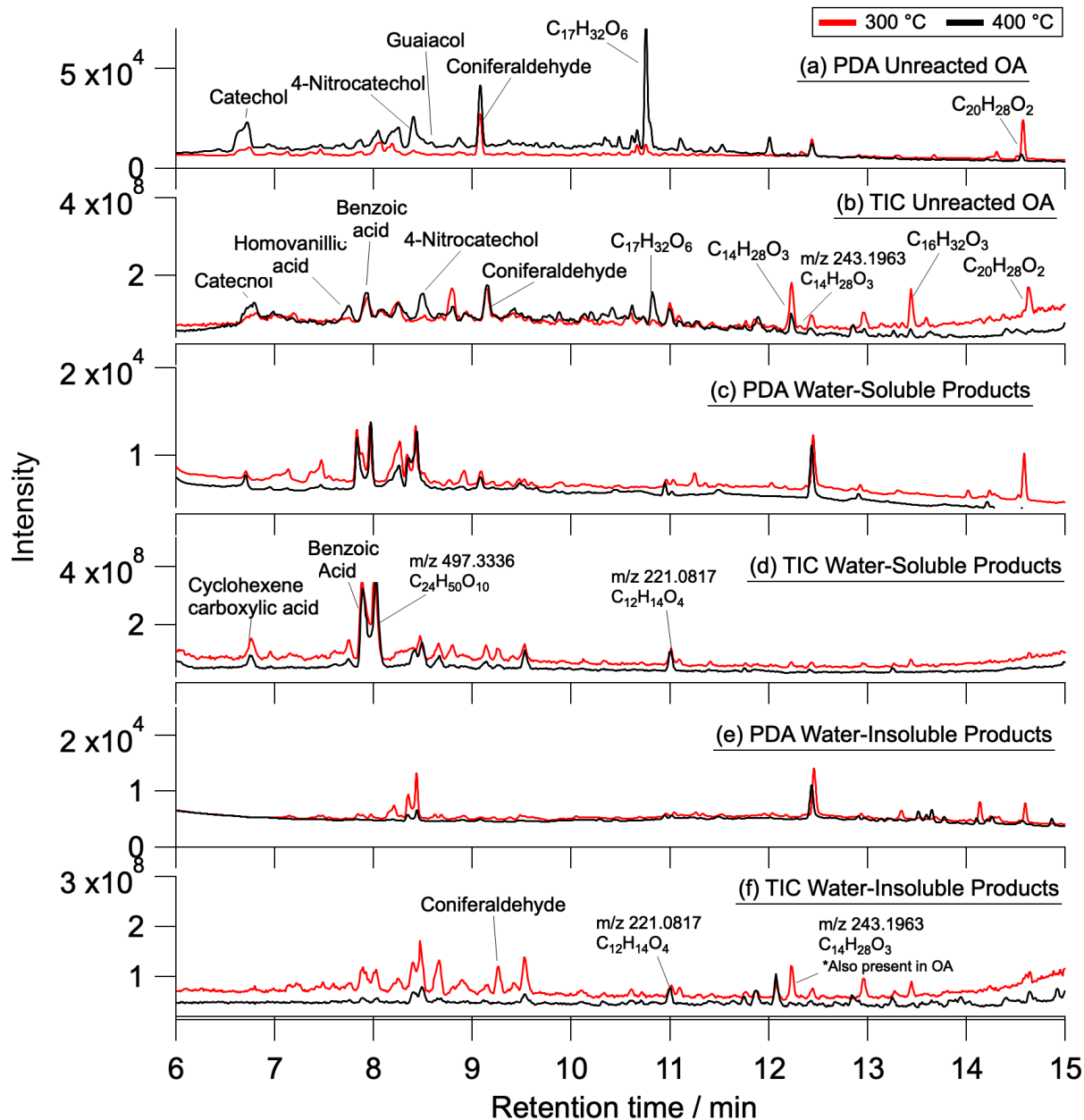


Figure S3. Sample UHPLC-PDA-HRMS chromatograms of reaction products for 300 °C (red) and 400 °C (black) OA + Fe(III). a) PDA chromatograms of unreacted OA; b) total ion chromatograms (TICs) of unreacted OA; c) PDA chromatograms of water-soluble OA + Fe(III) reaction products; d) TICs of water-soluble OA + FeCl₃ reaction products; e) PDA chromatograms of water-insoluble P300/400; and f) TICs of water-insoluble P300/400. P300 and P400 were filtered from the solution, redissolved in methanol, and rotary evaporated prior to analysis with HRMS. There is a 0.06-minute time delay between PDA and Orbitrap detectors. Unlabeled peaks in panel (b) can be identified using **Table S2**.

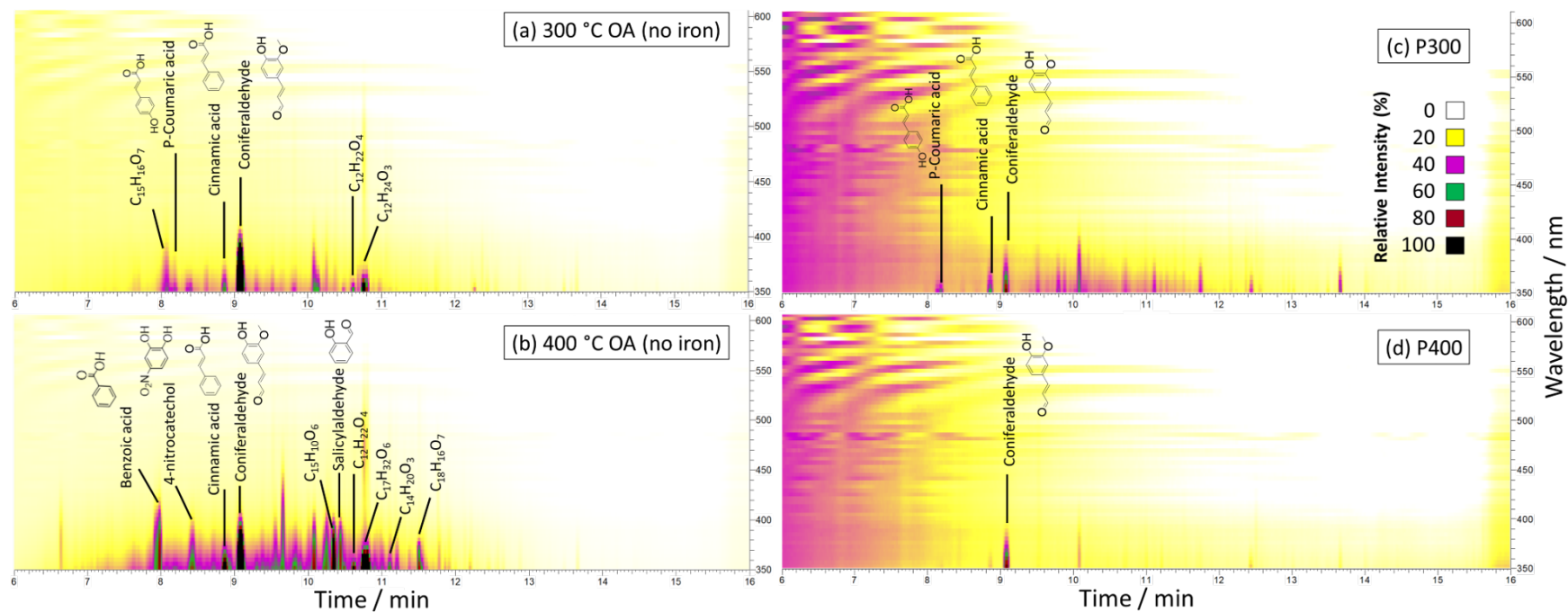


Figure S4. Heat maps of UHPLC-PDA chromatograms as a function of absorption wavelength for unreacted, water-soluble OA. The panels correspond to 300 °C (a) and 400 °C (b) data. Peaks were normalized to 5% of the largest peak intensity. Water-insoluble particles, P300 and P400 (panels c and d, respectively), were formed in the reaction of OA + Fe(III). Peaks were normalized to 100% of the largest peak intensity. In (a) and (b), coniferaldehyde is responsible for the 100% relative intensity of light absorption at 9.15 min. In (c) and (d), most light absorption species disappear except for the remaining coniferaldehyde.

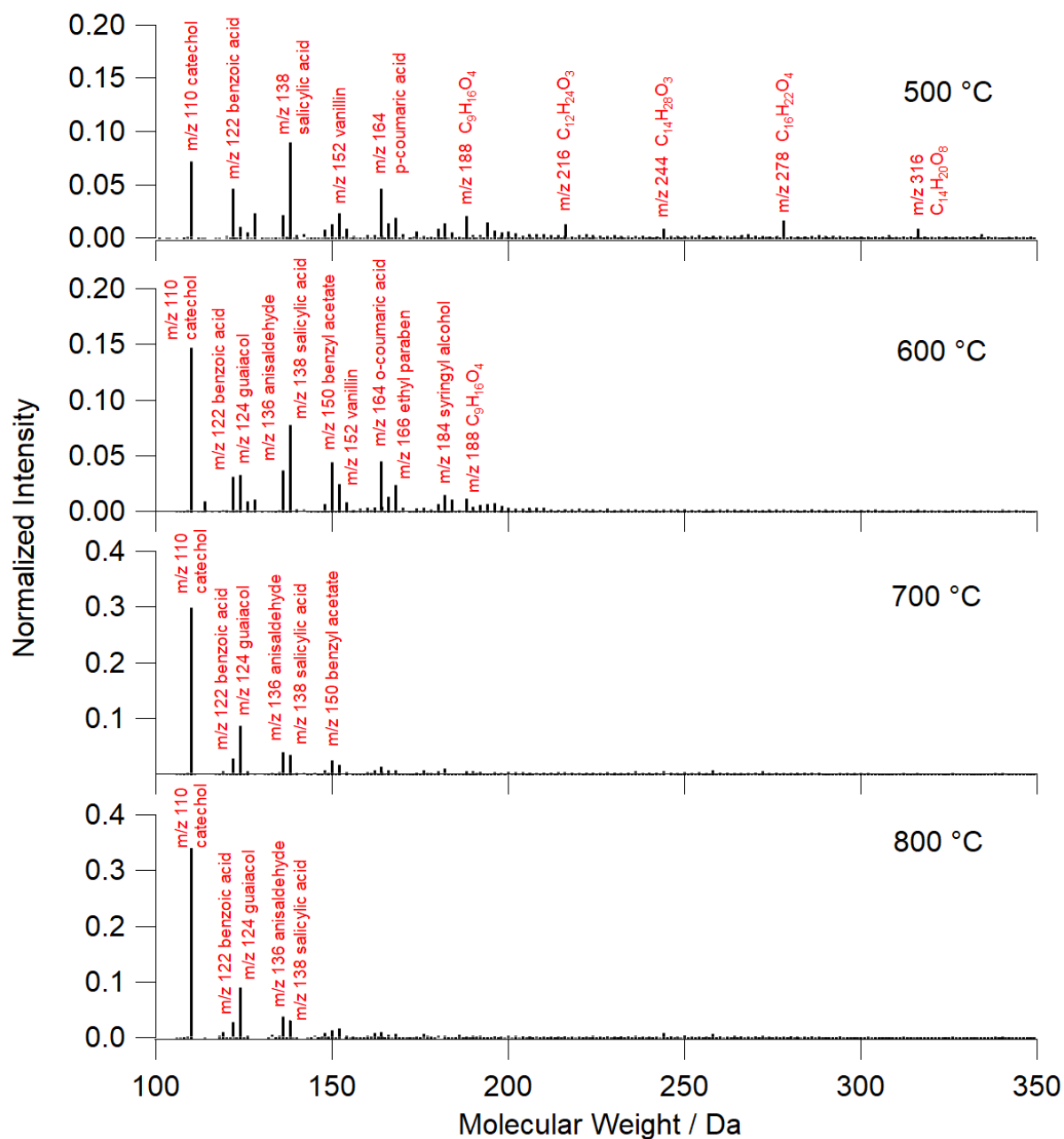


Figure S5. Mass spectra of OA500-800 samples run on UHPLC-PDA-HRMS prior to reaction with FeCl_3 . The X-axis corresponds to the molecular weight of the neutral compound (the m/z of observed ions corrected by the addition of the mass of a proton). Increasing pyrolysis temperature produced more water-insoluble PAH compounds. Smaller, less substituted compounds (catechol, benzoic acid, and guaiacol) were present at all temperatures but increasing pyrolysis temperature decreased the complexity of water-soluble species.

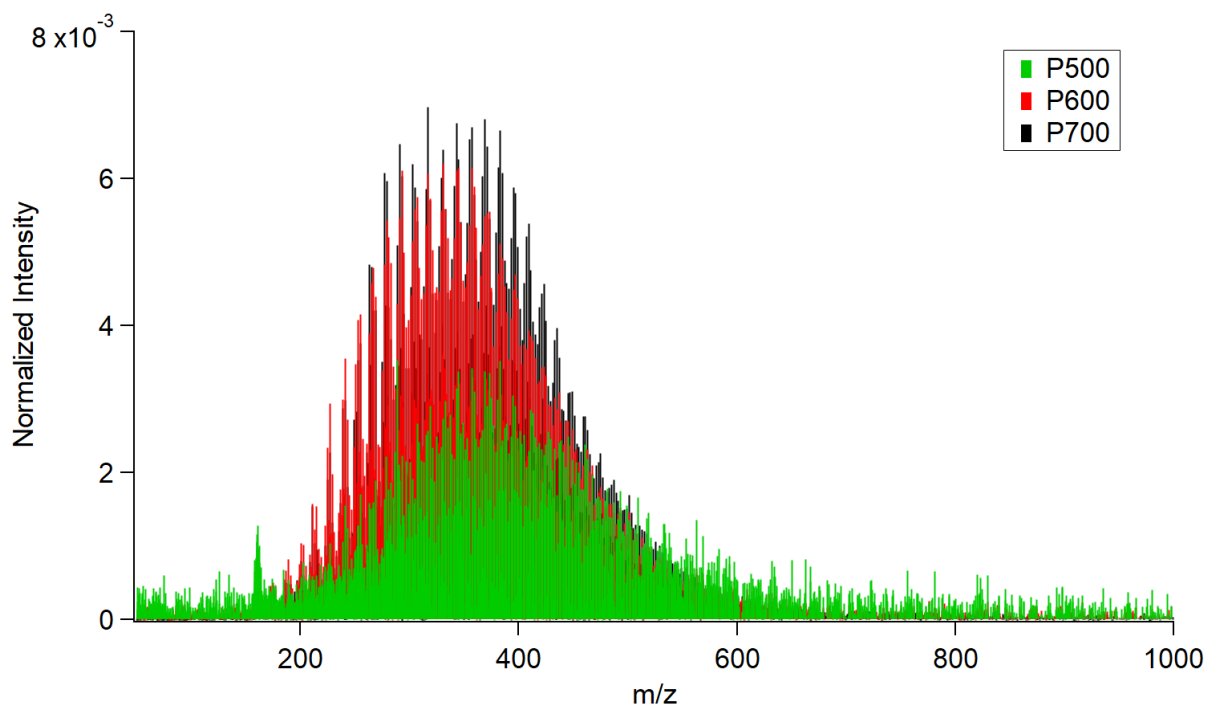


Figure S6. Laser desorption ionization time-of-flight mass spectrum (LDI-ToF-MS) for black water-insoluble particles. The colors correspond to P500 (green), P600 (red), and P700 (black) that were formed through the reaction of FeCl_3 with OA500-700. P800 was also run on LDI, however, particle concentration on the LDI plate was too low and the produced spectrum was noisy. Spectra were collected in negative ion mode with the assistance of Dr. Lisa Wingen and Dr. Ben Katz at the University of California, Irvine Mass Spectrometry Facility.

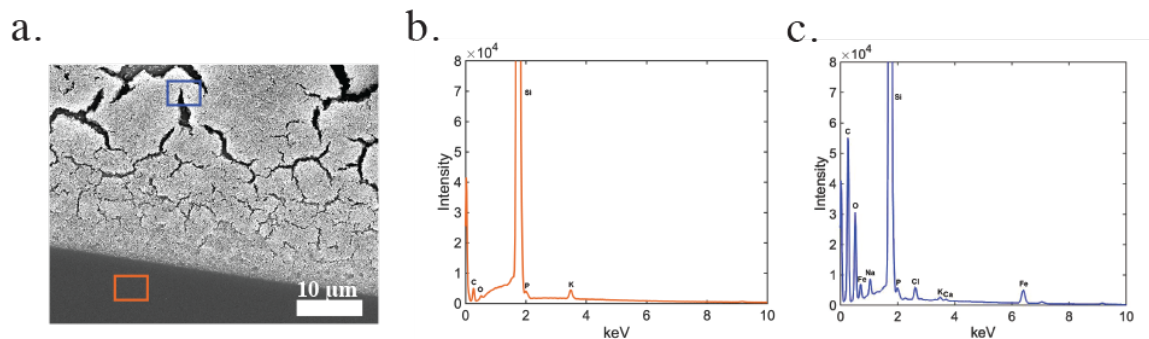


Figure S7. Representative SEM and EDS data for polycatechol particles. (a) SEM image of particles with the orange box indicates a blanked region scanned by EDS and the blue box indicates the sample region scanned by EDS. (b) EDS spectra of the blanked sample region, and (c) EDS spectra of the sample region.

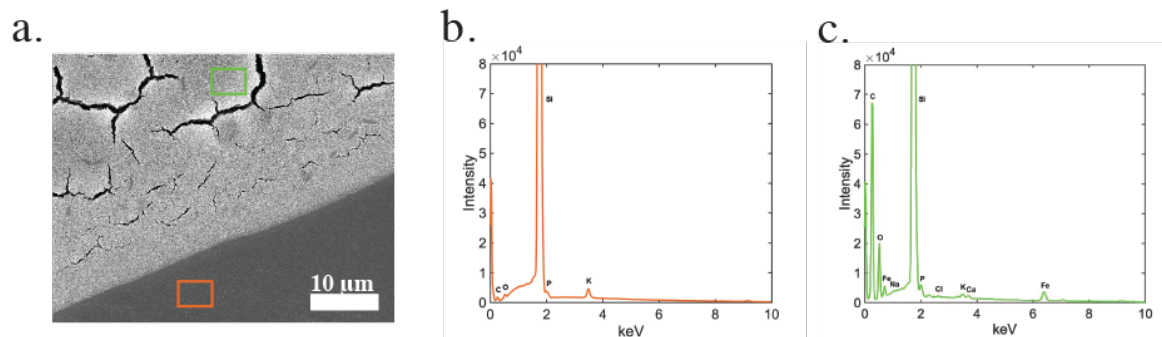
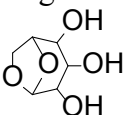
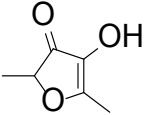
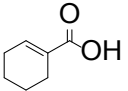
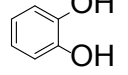
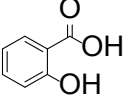
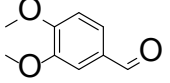
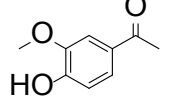
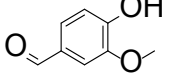
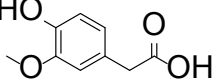
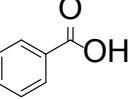
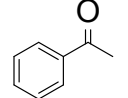
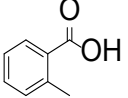
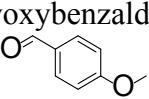
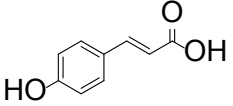
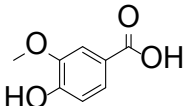
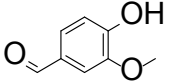
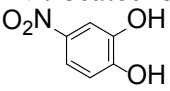
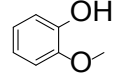


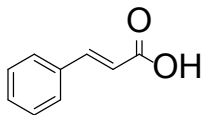
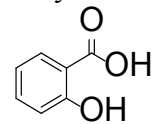
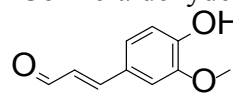
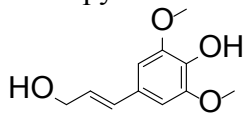
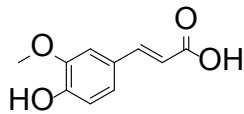
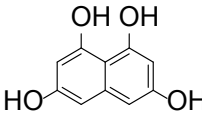
Figure S8. Representative SEM and EDS data for P600 (reaction particles) particles. (a) SEM particles with the orange box indicates a blanked region scanned by EDS and the blue box indicates the sample region scanned by EDS. (b) EDS spectra of the blanked sample region, and (c) EDS spectra of the sample region.

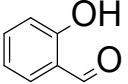
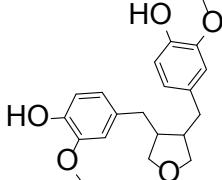
Table S2. List of compounds reproducibly detected by UHPLC-PDA-HRMS in negative ion mode from the pyrolysis of Canary Island Pine needles at 300-800 °C. The formulas of the neutral compounds were obtained by adding a proton to the ion formula, assuming that deprotonation was the main ionization mechanism. The normalized, relative peak abundances are designated for each temperature as “L” for Low (<5% peak abundance in time integrated mass spectra), “M” for Medium (6-14%), and “H” for High (15-100%). For light-absorbing species, tentative structural assignments were confirmed using absorption spectra recorded by the PDA detector. The last column shows the peak numbers that correspond to the red labeled numbers in **Figure 5** of the manuscript. Retention times without a number were also present on Figure 5 of the manuscript, but not labeled for simplicity.

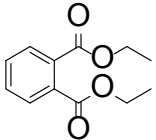
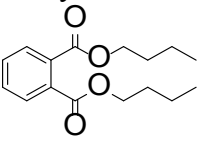
LC RT (min)	Observed <i>m/z</i>	Calculated <i>m/z</i>	Chemical Formula of Neutral Species	Tentative structures	300 °C	400 °C	500 °C	600 °C	700 °C	800 °C	References	Figure 5 peak numbers
1.46	161.0456	161.0455	C ₆ H ₁₀ O ₅	Levoglucosan 	L	L	L	L	L	L		
6.54	127.0401	127.0401	C ₆ H ₈ O ₃	Furaneol 			H	M				
6.71	125.0608	125.0608	C ₇ H ₁₀ O ₂	Cyclohexene carboxylic acid 	M	M	M	M	L	L	1	
6.60/6.82	109.0294	109.0295	C ₆ H ₆ O ₂	Catechol 	L	M	H	H	H	H	1,2	1
7.04	315.1085	315.1085	C ₁₄ H ₂₀ O ₈				M	L				

7.12	137.0242	137.0233	C ₇ H ₆ O ₃	Salicylic acid 		L	H	H	M	M		2
7.18	165.0558	165.0557	C ₉ H ₁₀ O ₃	Veratraldehyde  Acetovanillone 	L	L	L	M	L	L	1,3	3
7.32	151.0399	151.0389	C ₈ H ₈ O ₃	Vanillin 			L	H	L	L		4
7.68	181.0508	181.0506	C ₉ H ₁₀ O ₄	Homovanillic acid 	L	L	H	M	L	L	1,3,4	5
7.85/7.94	121.0294	121.0295	C ₇ H ₆ O ₂	Benzoic acid 	H	H	H	H	M	M	1,3-9	6
	283.1186	283.1187	C ₁₄ H ₂₀ O ₆			L						
8.07	173.0820	173.0819	C ₈ H ₁₄ O ₄		H							
8.14	307.0822	307.0823	C ₁₅ H ₁₆ O ₇		M							
8.25	119.0502	119.0502	C ₈ H ₈ O	Acetophenone 	M	M	L	L			7	

	135.0451	135.0452	C ₈ H ₈ O ₂	2-Methylbenzoic acid  Methoxybenzaldehyde 	H	H	H	H	M	M	4,5,10	8
	163.0401	163.0401	C ₉ H ₈ O ₃	p-Coumaric acid 	H	H	H	H	L		1,11	7
	167.0349	167.0350	C ₈ H ₈ O ₄	Vanillic acid 	M	M	H	L	L	L	1,3,4,12	8
	337.0927	337.0929	C ₁₆ H ₁₈ O ₈		L							
8.27	151.0401	151.0401	C ₈ H ₈ O ₃	Vanillin (isomer) 	L	M	H	H	L	L	1,3,13,14	
8.47	154.0145	154.0135	C ₆ H ₅ O ₄ N	4-Nitrocatechol 	L	M	L				15	9
8.52	123.0452	123.0452	C ₇ H ₈ O ₂	Guaiacol 	L	L	M	H	H	H	1,4,10,12	10
	293.1030	293.1031	C ₁₅ H ₁₈ O ₆		L	L	L					
8.79	187.0975	187.0976	C ₉ H ₁₆ O ₄		M	M	H	M	L	L		11

8.88	243.0661	243.0652	C ₁₄ H ₁₂ O ₄					L	M	M		12	
8.94	147.0451	147.0452	C ₉ H ₈ O ₂	Cinnamic acid 	H	H	M	L			1	13	
9.15/9.35	137.0243	137.0244	C ₇ H ₆ O ₃	3-hydroxybenzoic acid 	L	L	H	H	M	M	1,12	14	
	177.0557	177.0557	C ₁₀ H ₁₀ O ₃	Coniferaldehyde 	H	H	M	L			1,2,10,13,14	15	
	199.0975	199.0975	C ₁₀ H ₁₆ O ₄		H	M	M	L					
9.41	209.0818	209.0819	C ₁₁ H ₁₄ O ₄	Sinapyl alcohol 	M	M	L	L			12,16		
9.50	193.0507	193.0506	C ₁₀ H ₁₀ O ₄	Ferulic acid  1,3,6,8-Tetrahydroxynaphthalene 			H	L				14	16

9.76	149.0607	149.0597	C ₉ H ₁₀ O ₂			L	M	H	M	L		17
10.55	121.0295	121.0295	C ₇ H ₆ O ₂	Salicylaldehyde 		H						
10.58	185.0608	185.0597	C ₁₂ H ₁₀ O ₂						L	L		
10.68	287.2226	287.2227	C ₁₆ H ₃₂ O ₄		H	H	L					
	329.0665	329.0666	C ₁₇ H ₁₄ O ₇		M	H	L					18
10.72	229.1443	229.1445	C ₁₂ H ₂₂ O ₄		H	H	L					
	343.1548	343.1550	C ₂₀ H ₂₄ O ₅	Tetrahydro-3,4-divanillylfuran 		H	L					8
	375.1446	375.1449	C ₂₀ H ₂₄ O ₇			M	L					12
	421.1502	421.1504	C ₂₁ H ₂₆ O ₉		M	M						
10.82	285.0767	285.0768	C ₁₆ H ₁₄ O ₅			H						
	303.0872	303.0874	C ₁₆ H ₁₆ O ₆			M	L					
	331.2123	331.2126	C ₁₇ H ₃₂ O ₆			H						

10.97	215.1650	215.1652	C ₁₂ H ₂₄ O ₃		M	M	L	L	L	L		19
11.00	221.0816	221.0819	C ₁₂ H ₁₄ O ₄	Diethyl phthalate 	H	M	L	L			12,17	
	393.0613	393.0615	C ₂₁ H ₁₄ O ₈		M							
11.17	235.1339	235.1339	C ₁₄ H ₂₀ O ₃			M	L					
12.18/12.23	243.1963	243.1965	C ₁₄ H ₂₈ O ₃		H	H	M	L	L	L		20
12.43	293.1757	293.1747	C ₁₇ H ₂₆ O ₄		M	M	L					21
12.95	285.2069	285.2071	C ₁₆ H ₃₀ O ₄		H	M	L					
13.44	271.2275	271.2278	C ₁₆ H ₃₂ O ₃		H	M	L					22
13.89	277.1445	277.1445	C ₁₆ H ₂₂ O ₄	Dibutyl Phthalate 			H				5,17	23
14.38	249.1494	249.1496	C ₁₅ H ₂₂ O ₃		M							
14.64	299.2014	299.2016	C ₂₀ H ₂₈ O ₂		L	M						
	357.2068	357.2071	C ₂₂ H ₃₀ O ₄			L						
15.35	275.1649	275.1652	C ₁₇ H ₂₄ O ₃		H	M	L					
15.52	335.2227	335.2227	C ₂₀ H ₃₂ O ₄		M	L						

References

- 1 D. M. Smith, T. Cui, M. N. Fiddler, R. P. Pokhrel, J. D. Surratt and S. Bililign, Laboratory studies of fresh and aged biomass burning aerosol emitted from east African biomass fuels – Part 2: Chemical properties and characterization, *Atmos. Chem. Phys.*, 2020, **20**, 10169–10191.
- 2 H. Chin, K. S. Hopstock, L. T. Fleming, S. A. Nizkorodov and H. A. Al-Abadleh, Effect of aromatic ring substituents on the ability of catechol to produce brown carbon in iron(iii)-catalyzed reactions, *Environmental Science: Atmospheres*, 2021, **1**, 64–78.
- 3 D. R. Oros and B. R. T. Simoneit, Identification and emission factors of molecular tracers in organic aerosols from biomass burning Part 1. Temperate climate conifers, *Applied Geochemistry*, 2001, **16**, 1513–1544.
- 4 L. R. Mazzoleni, B. Zielinska and H. Moosmüller, Emissions of Levoglucosan, Methoxy Phenols, and Organic Acids from Prescribed Burns, Laboratory Combustion of Wildland Fuels, and Residential Wood Combustion, *Environ. Sci. Technol.*, 2007, **41**, 2115–2122.
- 5 L. T. Fleming, P. Lin, A. Laskin, J. Laskin, R. Weltman, R. D. Edwards, N. K. Arora, A. Yadav, S. Meinardi, D. R. Blake, A. Pillarsetti, K. R. Smith and S. A. Nizkorodov, Molecular composition of particulate matter emissions from dung and brushwood burning household cookstoves in Haryana, India, *Atmos. Chem. Phys.*, 2018, **18**, 2461–2480.
- 6 J. S. Smith, A. Laskin and J. Laskin, Molecular Characterization of Biomass Burning Aerosols Using High-Resolution Mass Spectrometry, *Anal. Chem.*, 2009, **81**, 1512–1521.
- 7 S. Tomaz, T. Cui, Y. Chen, K. G. Sexton, J. M. Roberts, C. Warneke, R. J. Yokelson, J. D. Surratt and B. J. Turpin, Photochemical Cloud Processing of Primary Wildfire Emissions as a Potential Source of Secondary Organic Aerosol, *Environ. Sci. Technol.*, 2018, **52**, 11027–11037.
- 8 D. R. Oros and B. R. T. Simoneit, Identification and emission factors of molecular tracers in organic aerosols from biomass burning Part 2. Deciduous trees, *Applied Geochemistry*, 2001, **16**, 1545–1565.
- 9 L. A. Edey and G. N. Richards, Analysis of condensates from wood smoke. Components derived from polysaccharides and lignins, *Environ. Sci. Technol.*, 1991, **25**, 1133–1137.
- 10 A. P. S. Hettiyadura, V. Garcia, C. Li, C. P. West, J. Tomlin, Q. He, Y. Rudich and A. Laskin, Chemical Composition and Molecular-Specific Optical Properties of Atmospheric Brown Carbon Associated with Biomass Burning, *Environ. Sci. Technol.*, 2021, **55**, 2511–2521.
- 11 B. R. T. Simoneit, W. F. Rogge, M. A. Mazurek, L. J. Standley, L. M. Hildemann and G. R. Cass, Lignin pyrolysis products, lignans, and resin acids as specific tracers of plant classes in emissions from biomass combustion, *Environ. Sci. Technol.*, 1993, **27**, 2533–2541.
- 12 L. T. Fleming, P. Lin, J. M. Roberts, V. Selimovic, R. Yokelson, J. Laskin, A. Laskin and S. A. Nizkorodov, Molecular composition and photochemical lifetimes of brown carbon chromophores in biomass burning organic aerosol, *Atmospheric Chemistry and Physics*, 2020, **20**, 1105–1129.
- 13 M. Loebel Roson, R. Duruisseau-Kuntz, M. Wang, K. Klimchuk, R. J. Abel, J. J. Harynuk and R. Zhao, Chemical Characterization of Emissions Arising from Solid Fuel Combustion—Contrasting Wood and Cow Dung Burning, *ACS Earth Space Chem.*, 2021, **5**, 2925–2937.
- 14 P. Lin, L. T. Fleming, S. A. Nizkorodov, J. Laskin and A. Laskin, Comprehensive Molecular Characterization of Atmospheric Brown Carbon by High Resolution Mass Spectrometry with

- Electrospray and Atmospheric Pressure Photoionization, *Anal. Chem.*, 2018, **90**, 12493–12502.
- 15 A. B. Dalton and S. A. Nizkorodov, Photochemical Degradation of 4-Nitrocatechol and 2,4-Dinitrophenol in a Sugar-Glass Secondary Organic Aerosol Surrogate, *Environ. Sci. Technol.*, 2021, **55**, 14586–14594.
- 16 B. R. T. Simoneit, Biomass burning — a review of organic tracers for smoke from incomplete combustion, *Applied Geochemistry*, 2002, **17**, 129–162.
- 17 S. Lee, K. Baumann, J. J. Schauer, R. J. Sheesley, L. P. Naeher, S. Meinardi, D. R. Blake, E. S. Edgerton, A. G. Russell and M. Clements, Gaseous and Particulate Emissions from Prescribed Burning in Georgia, *Environ. Sci. Technol.*, 2005, **39**, 9049–9056.